

Electronic Supplementary Information

Unraveling the effects of amino acid substitutions enhancing lipase resistance to an ionic liquid: a molecular dynamics study

Jing Zhao,^{ab} Victorine Josiane Frauenkron-Machedjou,^a Alexander Fulton,^c Leilei Zhu,^{ab}

Mehdi D. Davari,^a Karl-Erich Jaeger,^c Ulrich Schwaneberg,^{ad*} and Marco Bocola^{a*}

^a *Lehrstuhl für Biotechnologie, RWTH Aachen University, Worringerweg 3, 52074 Aachen, Germany*

^b *Tianjin Institute of Industrial Biotechnology, Chinese Academy of Sciences, 300308 Tianjin, China*

^c *Institute of Molecular Enzyme Technology, Heinrich-Heine-University Düsseldorf, Forschungszentrum Jülich, 52426 Jülich, Germany*

^d *DWI-Leibniz Institute for Interactive Materials, Forckenbeckstraße 50, 52056 Aachen, Germany*

*Corresponding authors:

Prof. Dr. Ulrich Schwaneberg

RWTH Aachen University, Lehrstuhl für Biotechnologie, Worringerweg 3, 52074 Aachen, Germany

Tel.: +49-241-80 24176, Fax: +49-241-80 22387

E-Mail: u.schwaneberg@biotec.rwth-aachen.de

Dr. Marco Bocola

RWTH Aachen University, Lehrstuhl für Biotechnologie, Worringerweg 3, 52074 Aachen, Germany

Tel.: +49-241-80 24170, Fax: +49-241-80 22387

E-Mail: m.bocola@biotec.rwth-aachen.de

Table S1 Summary of the selected resistant and non-resistant BSLA single variants.

Variant	Secondary structure ^a	Location ^b	Distance of S77 O _γ to C _β of mutated residue (Å) ^c	Minimal distance of mutated residue to substrate-binding cleft (Å) ^d	Hydrophobic index change ^e
P5F	Coil	Buried	23.1	17.0	146
P5M	Coil	Buried	23.1	17.6	120
I12Q	Turn	Exposed	6.0	0.0	-109
I12R	turn	Exposed	6.0	0.0	-113
F17V	3/10-helix	Exposed	15.5	1.4	-24
N18E	3/10-helix	Exposed	10.2	0.0	-3
K23W	α-helix	Exposed	18.6	6.7	120
K23I	α-helix	Exposed	18.6	7.8	122
D34K	3/10-helix	Exposed	27.4	17.8	32
D34R	3/10-helix	Exposed	27.4	16.9	41
L36P	N-terminal β-strand	Exposed	20.4	13.0	-143
L36D	N-terminal β-strand	Exposed	20.4	12.6	-152
G46E	Coil	Exposed	27.0	4.1	-31
T47H	Coil	Exposed	13.6	5.0	-5
G52D	α-helix	Buried	20.3	11.1	-55
V54K	α-helix	Exposed	16.6	11.2	-99
R57Y	α-helix	Exposed	21.9	15.6	77
E65P	α-helix	Exposed	28.0	20.0	-15
M78Q	N-terminal α-helix	Exposed	4.7	0.0	-84
M78N	N-terminal α-helix	Exposed	4.7	0.0	-102
A81W	α-helix	Buried	8.5	2.9	56
A81R	α-helix	Buried	8.5	3.0	-55
A81E	α-helix	Buried	8.5	3.6	-72
T83D	α-helix	Buried	11.9	7.2	-68
L84D	α-helix	Buried	13.3	6.9	-152
K88R	α-helix	Exposed	18.6	6.8	9
L90D	bend	Exposed	20.2	14.2	-152

D91R	bend	Exposed	23.9	16.0	41
D91W	bend	Exposed	23.9	16.0	152
D91Y	bend	Exposed	23.9	16.6	118
D91M	bend	Exposed	23.9	17.3	129
A97D	β -strand	Exposed	23.0	14.8	-96
T109I	Turn	Exposed	12.8	1.4	86
T109E	Turn	Exposed	12.8	1.4	-44
A132Q	Turn	Exposed	14.2	4.6	-51
A132K	Turn	Exposed	14.2	4.4	-64
I135R	Bend	Exposed	5.9	0.0	-113
V136N	Bend	Exposed	5.4	0.0	-104
M137P	Coil	Exposed	11.1	1.3	-120
M137H	Coil	Exposed	11.1	1.3	-66
D144F	β -bridge	Exposed	19.9	8.0	155
G145F	Turn	Exposed	28.2	11.7	100
G145Q	Turn	Exposed	28.2	10.8	-10
R147E	N-terminal β -strand	Exposed	19.7	11.7	-17
I151E	C-terminal β -strand	Buried	15.8	7.5	-130
V154H	Coil	Exposed	13.4	4.5	-68
L159D	3/10-helix	Buried	8.9	1.3	-152
V165E	α -helix	Buried	13.9	6.0	-107
N166E	α -helix	Exposed	18.0	6.8	-3
S167V	α -helix	Exposed	20.9	8.6	81

Non-resistant BSLA variants

I12F	Turn	Exposed	6.0	0.0	1
K23E	α -helix	Exposed	18.6	7.2	-8
D34F	3/10-helix	Exposed	27.4	16.0	155
D34M	3/10-helix	Exposed	27.4	15.8	129
L36W	N-terminal β -strand	Exposed	20.4	12.3	0
G46M	Coil	Exposed	27.0	4.0	74
L135F	Bend	Exposed	5.9	0.0	3
V136E	Bend	Exposed	5.4	0.0	-107
I151W	C-terminal β -strand	Buried	15.8	8.6	-2

V165K	α -helix	Buried	13.9	7.4	-99
-------	-----------------	--------	------	-----	-----

^a The secondary structure of the mutated residue was defined by DSSP program, and no structure was defined as “coil”.

^b The exposed residue was defined when its accessible surface area was $> 5\%$ (using a “water” radius of 1.5 Å).

^c For Gly, one hydrogen atom was added to C α , and the distance of second HA atom to S77 O γ was determined. The crystal structure of BSLA wild-type (PDB code: 1I6W, chain A) ¹ was used for analysis.

^d The substrate-binding site was defined by the distances of surface atoms in binding cleft within 10 Å from S77 O γ . It includes G11, I12, G13, G14, N18, H76, S77, M78, A105, L108, I135, V136, L140, H156, I157, L160 and Y161. The last snapshot of MD simulation in water for each variant was used for analysis.

^e Hydrophobic index change was calculated by hydrophobic index (variant) - hydrophobic index (wild-type), in which the hydrophobic index of each amino acid at pH 7 was taken from the literature ². The values for each amino acid are normalized so that the most hydrophobic residue is given a value of 100 relative to glycine.

Table S2 The possible mechanisms explaining the selected resistant and non-resistant BSLA variants in 15 vol% [Bmim][TfO].

Resistant variant	Resistant mechanism	non-resistant variant	Non-resistant mechanism
I12R (surface)	– Surface residue became more polar; – Positively charged substrate-binding cleft, reducing the probability of [Bmim] ⁺ near the cleft	I12F (surface)	– Hydrophobic interaction of F12 with I135, blocking the substrate-binding cleft; – Accumulation of [Bmim] ⁺ by π - π interaction with phenol ring of F12
K23I (surface)	Stronger hydrophobic interaction with surrounding residues, e.g., F19, A20, I22, L26, V27, L36	K23E (surface)	– One additional salt-bridge E23-R33, rearranging the local structure; – Less interaction with surrounding nonpolar residues
D34R (surface)	One additional salt-bridge R34-E65	D34F (surface)	– Exposed hydrophobic side-chain; – Surrounding residues are polar, e.g., S32, R33, K35
D34R (surface)	One additional salt-bridge R34-E65	D34L (surface)	– Exposed hydrophobic side-chain; – Surrounding residues are polar, e.g., S32, R33, K35
L36D (surface)	One additional salt-bridge D36-K23	L36W (surface)	– Larger hydrophobic side-chain; – Surrounding residues are polar, e.g., K23, S32, R33, D34, K35, Y37
G46E (surface)	– Surface residue became more polar; – The loop where E46 located moved towards the substrate binding cleft, yielding more polar cleft	G46M (surface)	Exposed larger hydrophobic side-chain
I135R (surface)	– Surface residue became more polar; – Positively charged substrate-binding cleft, reducing the probability of [Bmim] ⁺ near the cleft	I135F (surface)	– Hydrophobic interaction of I12 with F135, blocking the substrate-binding cleft – [Bmim] ⁺ clustered near substrate-binding cleft
V136N (surface)	– One additional H-bond: N136-S141; – Substrate-binding cleft became more polar	V136E (surface)	H-bond network of active site was lost
I151E (Buried)	One additional H-bond: E151-Q164	I151W (Buried)	– H-bond network of active site was lost; – Interaction with surrounding IL ions, and π - π interaction of W151-H152, changing the loop structure where active site residue H156 located
V165E (Buried)	Two additional H-bonds: E165-Q164 & E165-S162	V165K (Buried)	– H-bond network of active site was lost; – α -helix structure where K165 located was changed

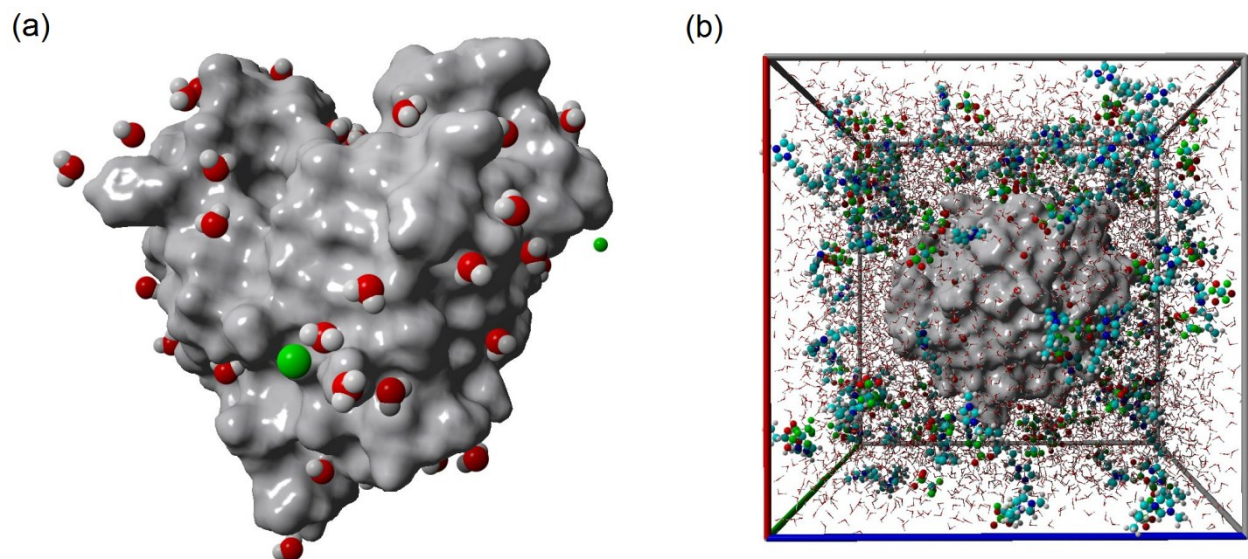


Fig. S1 (a) Structure of the simulated solute BSLA, with surface water molecules and five chlorine counterions (green) which are within 3 Å from protein. The enzyme surface is shown in grey. (b) An example of BSLA solvated in 15 vol% [Bmim][TfO], with cations and anions shown in ball stick, and water molecules in stick.

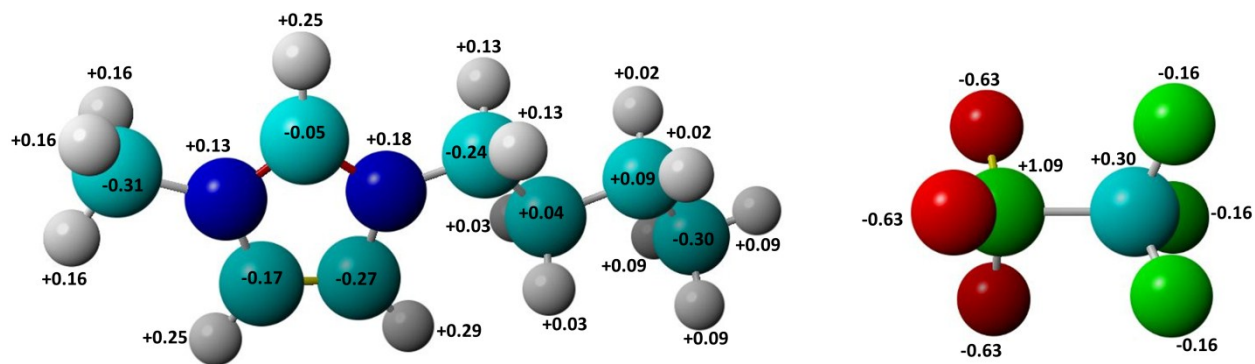
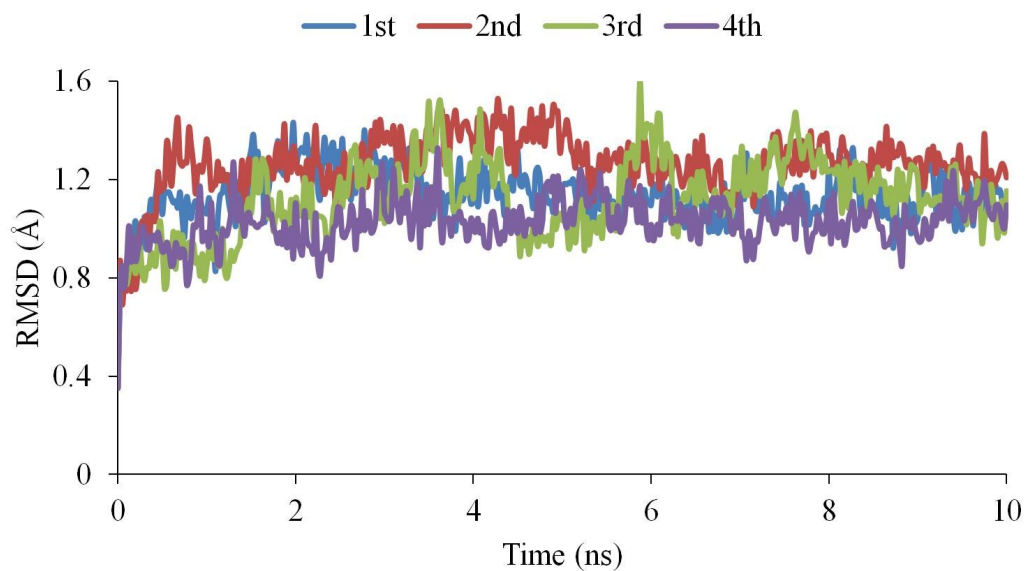


Fig. S2 The structure and partial charges of [Bmim][TfO] that were used in the force field for all MD simulations. The partial charges were calculated at the HF/6-31G(d) level^{3,4}.

(a) Backbone RMSD in water



(b) Backbone RMSD in 15 vol% [Bmim][TfO]

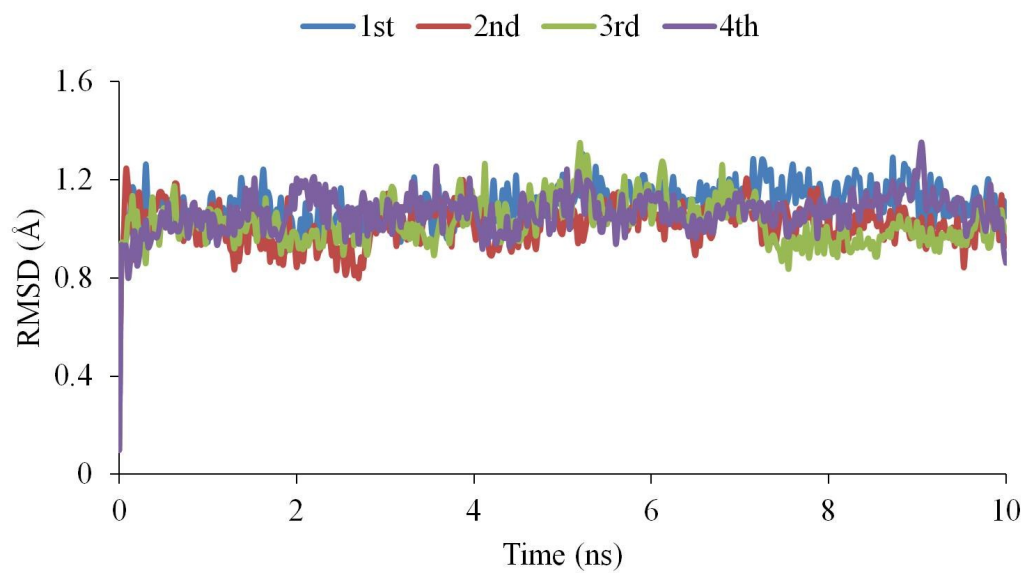


Fig. S3 The backbone RMSD of wild-type in water (a) and 15 vol% [Bmim][TfO] (b) from the starting structure. Four independent simulation runs were performed.

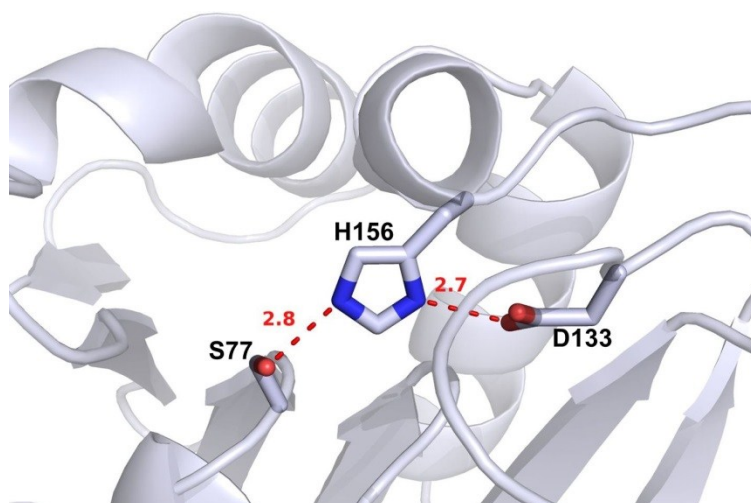


Fig. S4 The hydrogen bond network in the BSLA active site (PDB code: 1I6W, chain A) (van Pouderoyen et al. 2001). The side chains of the catalytic triad (S77, D133 and H156) are represented in stick. The hydrogen bonds are shown by red dashed line (distance shown besides the line in Å). Two crucial hydrogen bonds: (S77-H156) (hydroxyl oxygen of S77 and imidazole nitrogen of H156), and (D133-H156) (carboxylate oxygen of D133 and imidazole nitrogen of H156).

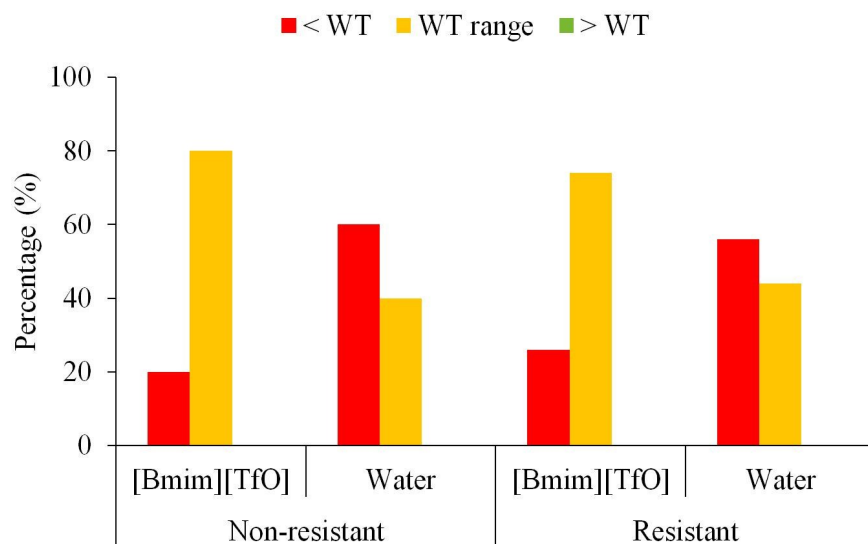
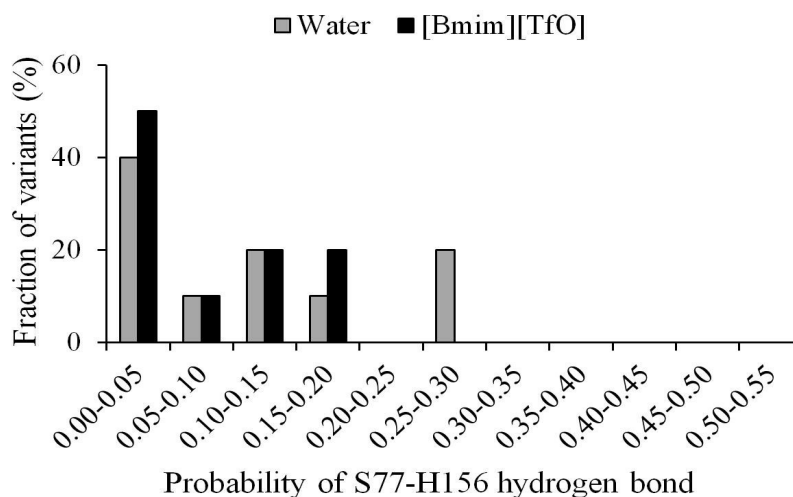
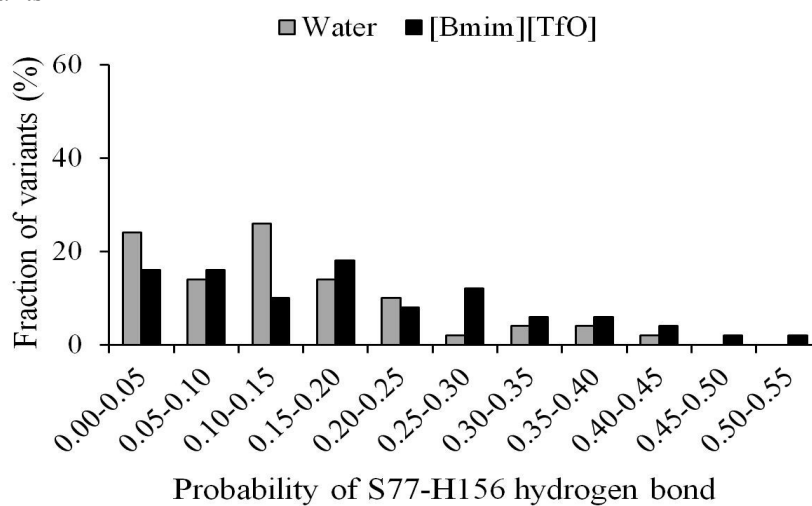


Fig. S5 Probability of D133-H156 hydrogen bond for resistant and non-resistant BSLA variants in water and 15 vol% [Bmim][TfO] systems. The percentage numbers indicate the fraction of the variants exhibiting higher (green), within wild-type deviation (yellow), and lower (red) probability of D133-H156 hydrogen bond compared with wild-type.

(a) Non-resistant variants



(b) Resistant variants



(c) Wild-type

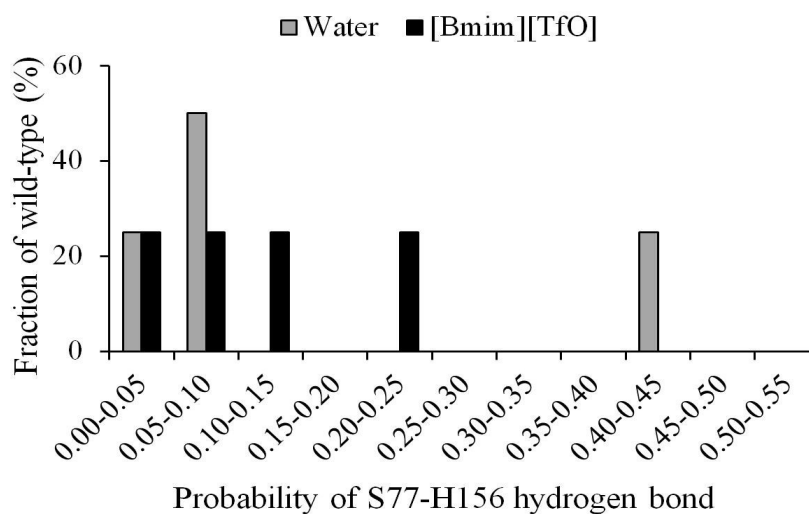
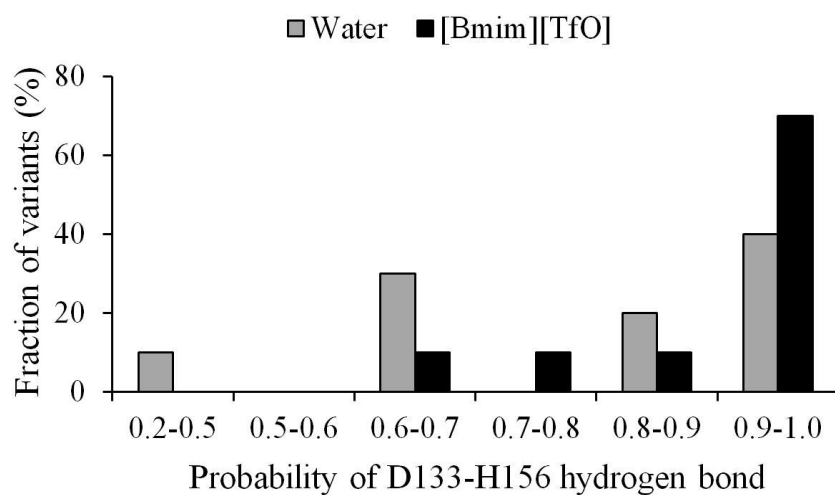
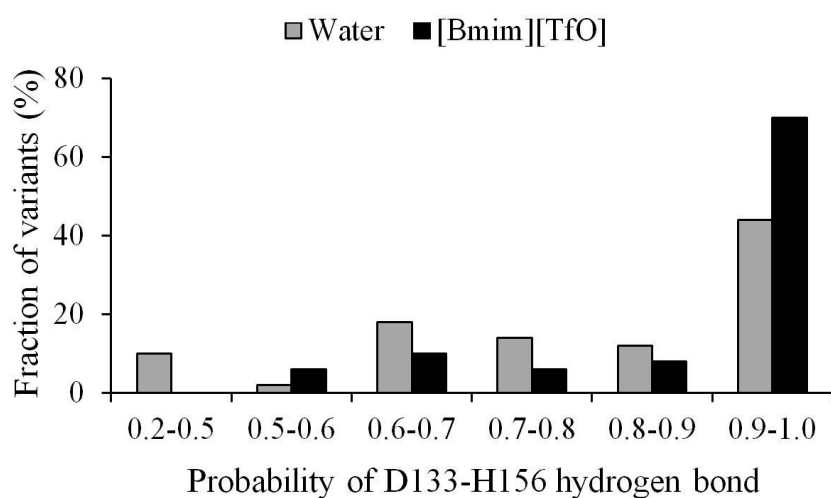


Fig. S6 Histograms of probability of S77-H156 hydrogen bond for non-resistant (a), resistant variants (b) and wild-type (c) in water and 15 vol% [Bmim][TfO] systems.

(a) Non-resistant variants



(b) Resistant variants



(c) Wild-type

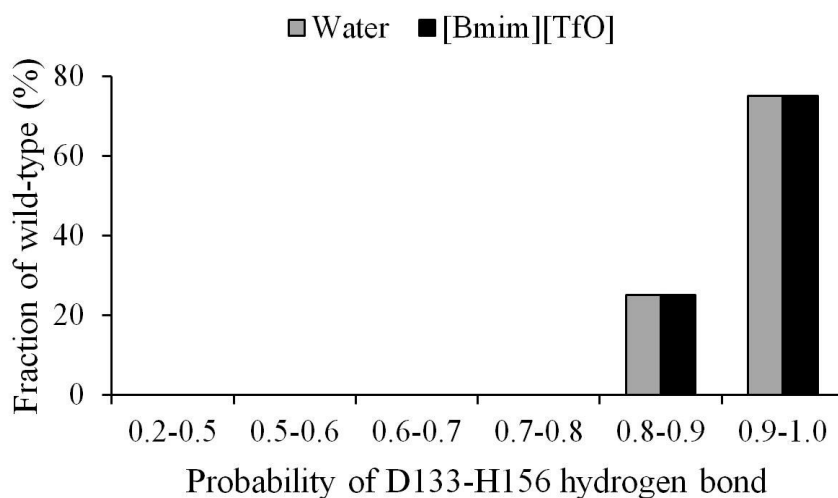


Fig. S7 Histograms of probability of D133-H156 hydrogen bond for non-resistant (a), resistant variants (b) and wild-type (c) in water and 15 vol% [Bmim][TfO] systems.

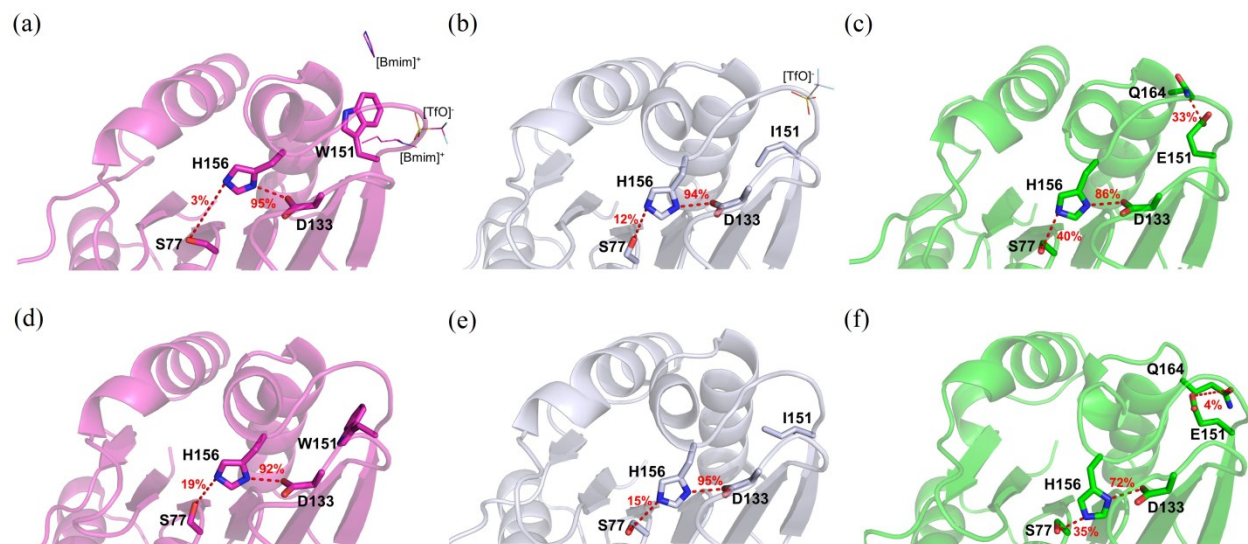


Fig. S8 Hydrogen bond networks of the catalytic triad for non-resistant variant I151W, wild-type, and resistant variant I151E in 15 vol% [Bmim][TfO] and water systems. (a) I151W in 15 vol% [Bmim][TfO]; (b) wild-type in 15 vol% [Bmim][TfO]; (c) I151E in 15 vol% [Bmim][TfO]; (d) I151W in water; (e) wild-type in water; (f) I151E in water. The probabilities of hydrogen bonds, calculated over the last 5 ns trajectories from three (four in the case of wild-type) independent simulations, are shown besides the dashed line. The structures of last snapshots are shown. The ionic liquid ions that are within 5 Å from residue 151 are shown in line. All protein orientations are identical to facilitate comparison.

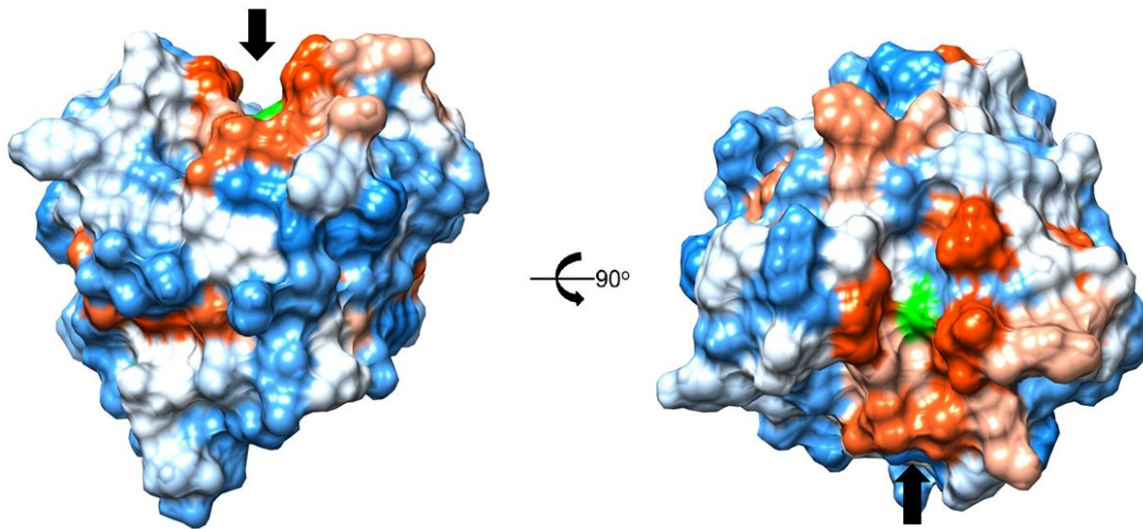
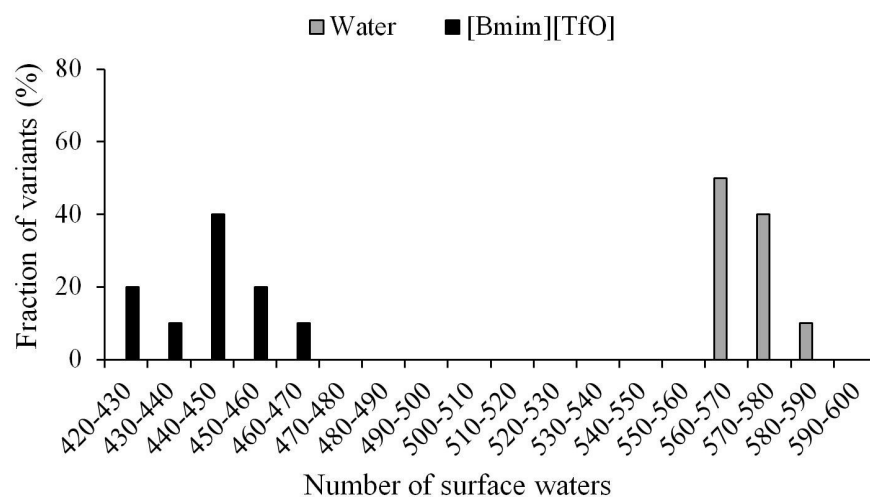
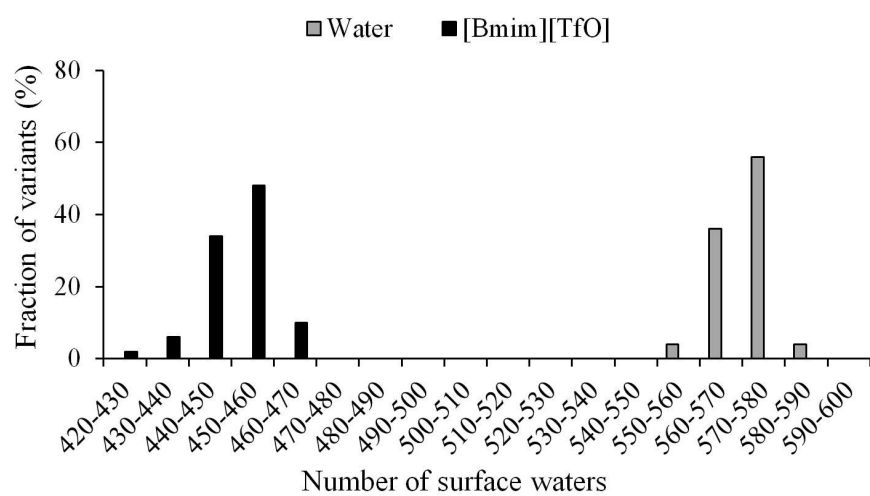


Fig. S9 The polarity and shape of substrate-binding cleft in the crystal structure of BSLA wild-type (PDB code: 1I6W, chain A). The surface of catalytic residue S77 is represented by green, and other residues are colored from hydrophobic (orange) to hydrophilic (blue). The substrate-binding cleft is indicated by the black arrow.

(a) Non-resistant variants



(b) Resistant variants



(c) Wild-type

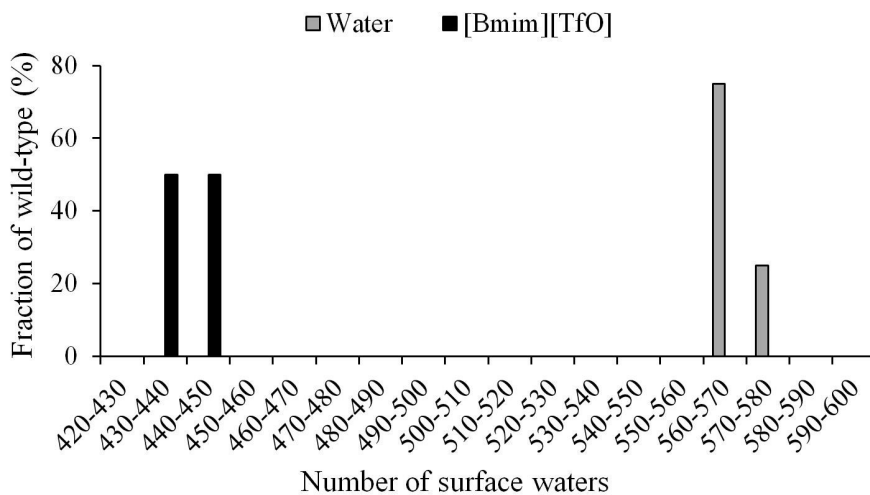
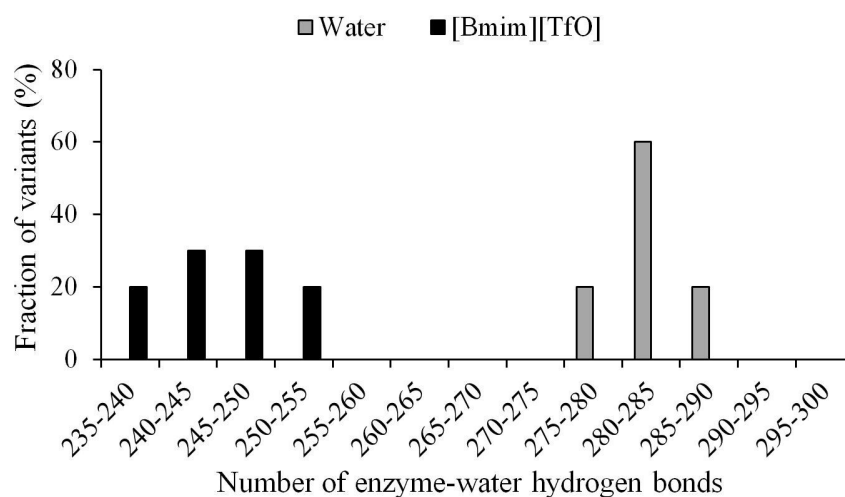
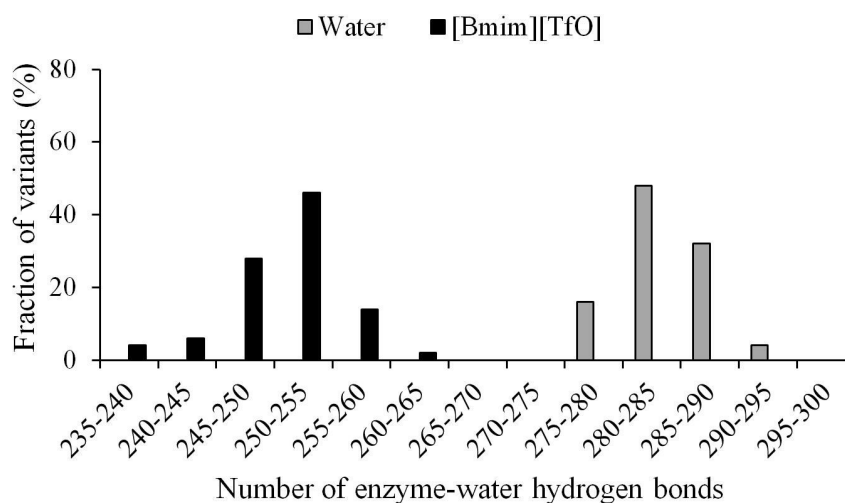


Fig. S10 Histograms of number of surface waters (within 3 Å from enzyme surface) for non-resistant (a), resistant variants (b) and wild-type (c) in water and 15 vol% [Bmim][TfO] systems.

(a) Non-resistant variants



(b) Resistant variants



(c) Wild-type

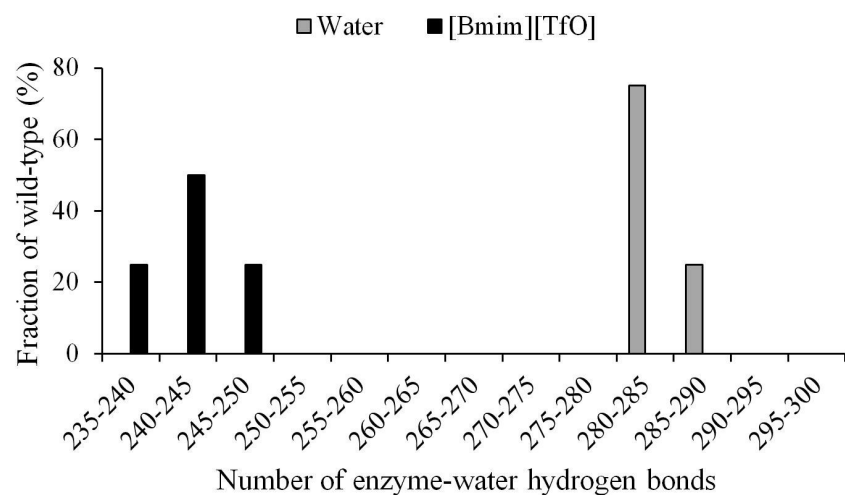
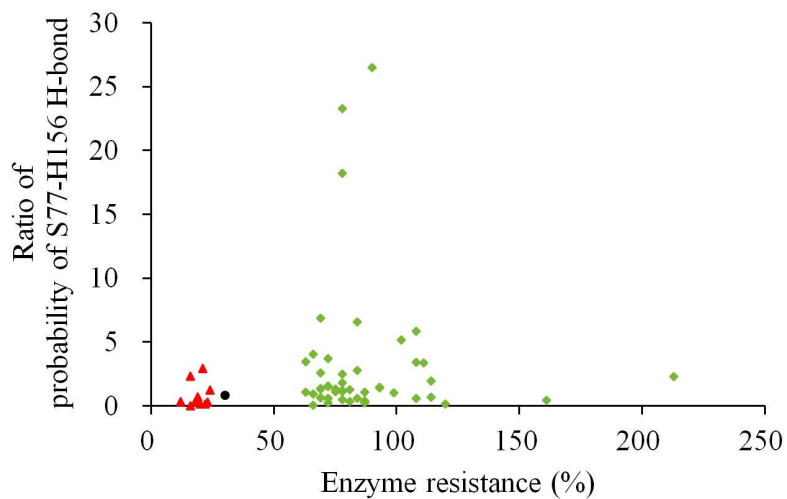
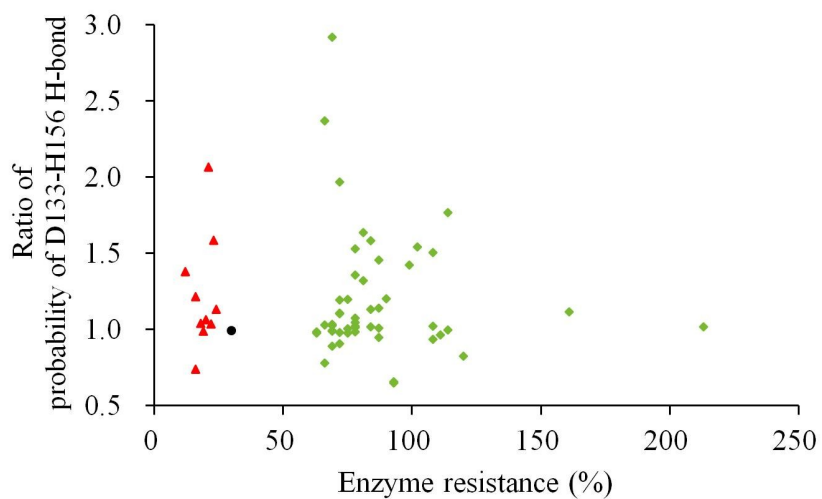


Fig. S11 Histograms of number of hydrogen bonds between enzyme and waters for non-resistant (a), resistant variants (b) and wild-type (c) in water and 15 vol% [Bmim][TfO] systems.

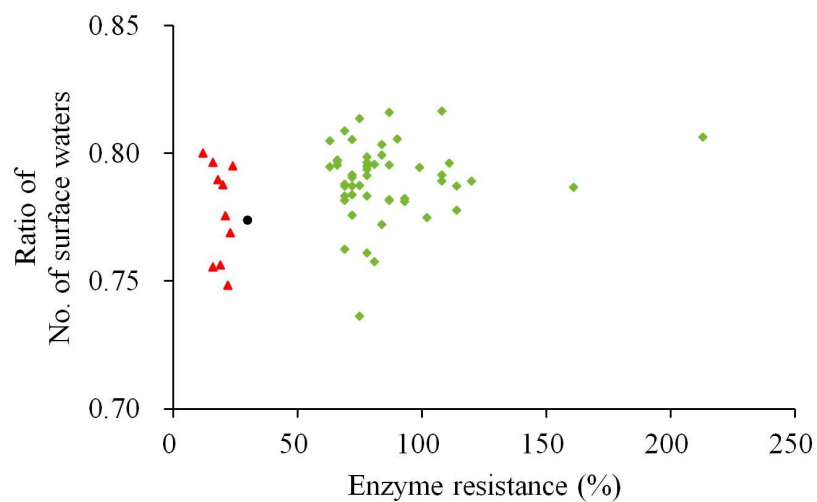
(a) Probability of S77-H156 hydrogen bond



(b) Probability of D133-H156 hydrogen bond



(c) Number of surface waters



(d) Number of hydrogen bonds between enzyme and waters

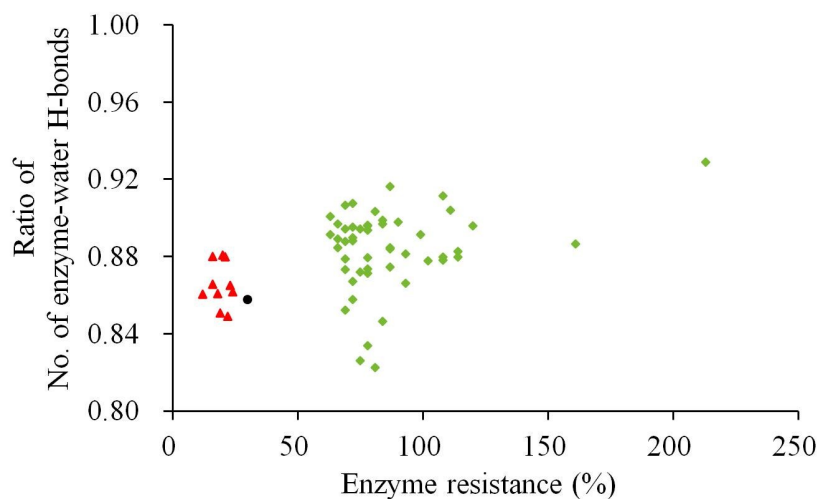


Fig. S12 Correlations between enzyme resistance and the analyzed properties. (a) Probability of S77-H156 hydrogen bond; (b) Probability of D133-H156 hydrogen bond; (c) Number of surface waters; (d) Number of hydrogen bonds between enzyme and waters. The ratio of the analyzed property (Y-axis) was calculated by the value of specific property in 15 vol% [Bmim][TfO] divided by that in water. Taken (a) as an example, the ratio value of each BSLA = probability of S77-H156 hydrogen bond of each BSLA in 15 vol% [Bmim][TfO] / respective probability in water. Green diamond: resistant variants; Red triangle: non-resistant variants; Black circle: wild-type.

References:

1. G. van Pouderoyen, T. Eggert, K. E. Jaeger and B. W. Dijkstra, *J. Mol. Biol.*, **2001**, 309, 215-226.
2. O. D. Monera, T. J. Sereda, N. E. Zhou, C. M. Kay and R. S. Hodges, *J. Pept. Sci.*, **1995**, 1, 319-329.
3. P. C. Hariharan and J. A. Pople, *Theor. Chim. Acta*, **1973**, 28, 213-222.
4. W. J. Hehre, R. Ditchfield and J. A. Pople, *J. Chem. Phys.*, **1972**, 56, 2257-2261.